

# Sensitive measurements of electric field distributions in low-pressure Ar plasmas by laser-induced fluorescence-dip spectroscopy

K. Takizawa,<sup>a)</sup> K. Sasaki,<sup>b)</sup> and A. Kono

Department of Electronics, Nagoya University, Nagoya 464-8603, Japan

(Received 27 August 2003; accepted 18 November 2003)

Laser-induced fluorescence-dip (LIF-dip) spectroscopy of Ar was used for measuring the distributions of sheath electric fields in low-pressure, inductively-coupled Ar plasmas. A sensitive detection limit of 3 V/cm obtained by LIF-dip allowed the measurement in the presheath region. The distributions of electric fields observed experimentally were compared with those of theoretical calculations based on a simple fluid model. As a result, reasonable agreement between the experiment and the theory was obtained in the electric fields in the sheath region, while the electric fields in the presheath region observed experimentally were higher than the theoretical results. © 2004 American Institute of Physics. [DOI: 10.1063/1.1639943]

The measurement of sheath electric field is an important task for optimizing plasma processing of materials. This is because the electric field in the sheath region between a bulk plasma and a material plays essential roles. For example, in plasma etching, positive ions are accelerated toward a wafer by the sheath electric field to obtain an anisotropic etching profile. However, in spite of the importance of the sheath electric field, its detailed structure has not been investigated well. In particular, the structure of the electric field in the presheath region is an open question. Since charged particles are extracted from a plasma toward a material via the presheath, the knowledge on the electric field in the presheath region is essential for the basic understanding of plasma processing tools.

Reliable diagnostics with high sensitivity and sufficient resolution are necessary for the precise measurement of the electric field in the sheath and presheath regions. Laser-aided Stark spectroscopy is a reliable method with a fine resolution. However, a typical detection limit of conventional Stark spectroscopy such as laser optogalvano spectroscopy<sup>1</sup> and laser-induced collisional-fluorescence spectroscopy<sup>2,3</sup> is roughly 500 V/cm, which is not sufficient for measuring the electric field in the presheath region. In addition, conventional Stark spectroscopy has limitations in the discharge pressure and the discharge geometry. Recently, we have applied laser-induced fluorescence-dip (LIF-dip) spectroscopy<sup>4</sup> to Ar, and have achieved a sensitive detection limit of 6 V/cm.<sup>5</sup> This method has no limitations in the gas pressure and the discharge geometry. In the present work, we have used LIF dip of Ar for measuring the distributions of the electric fields in the sheath and presheath regions of low-pressure Ar plasmas.

Figure 1 shows the experimental apparatus. A one-turn rf antenna (a diameter of 50–60 mm) covered with an insulator was inserted into a stainless-steel chamber of an internal diameter of 100 mm, and was connected to a rf power source at a frequency of 13.56 MHz via a matching circuit. Argon gas was injected from the top of the vacuum chamber, and

was evacuated from the bottom of the chamber. The gas pressure was measured using a capacitance manometer. A planar electrode (a diameter of 40 mm), which was movable along the vertical direction, was installed at the center of the chamber. The distance between the rf antenna and the electrode was set at 80 and 50 mm in the high- and low-density operations, respectively. The electrode was connected to a dc power supply. The strength of the electric field as a function of the distance from the electrode surface was measured by moving the electrode.

The excitation and observation scheme of LIF dip of Ar has been described in a previous article.<sup>5</sup> Briefly, this scheme employs two tunable lasers to excite Ar atoms at the metastable  $4s[3/2]_2^o$  state to high Rydberg states. The first tunable laser at a wavelength of 763.51 nm excite the  $4s[3/2]_2^o$  state to the  $4p[3/2]_2$  state. The  $4p[3/2]_2$  state populated by the first-step excitation is excited to high Rydberg states by the second tunable laser. By sweeping the wavelength of the second tunable laser, the spectral distribution of a Rydberg state influenced by Stark effect is observed as the dip spectrum of the laser-induced fluorescence at 800.62 nm from the  $4p[3/2]_2$  to  $4s[3/2]_1^o$  states. The strength of the electric field can be determined from the dip spectrum.

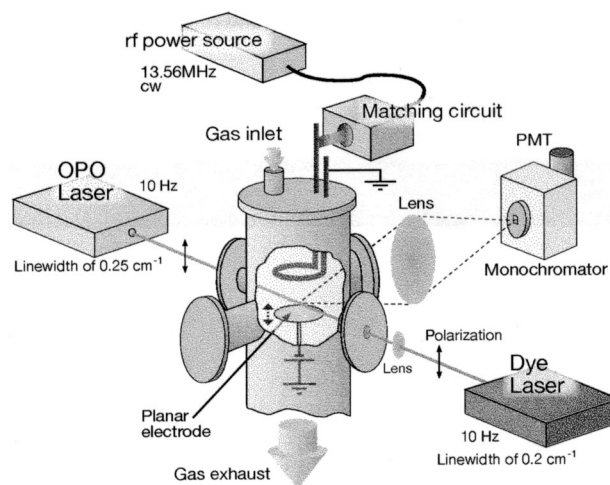


FIG. 1. Experimental apparatus.

<sup>a)</sup>Electronic mail: k-takiza@echo.nuee.nagoya-u.ac.jp

<sup>b)</sup>Electronic mail: sasaki@nuee.nagoya-u.ac.jp

In the present experiment, we used a dye laser pumped by an excimer laser and an optical parametric oscillator (OPO) pumped by a Nd:YAG laser for the first and second step excitations, respectively. The repetition rates of the laser pulses were 10 Hz. The spectral linewidths of the dye and OPO lasers were 0.2 and 0.25  $\text{cm}^{-1}$ , respectively. The polarizations of the two tunable lasers were parallel to the normal direction of the electrode surface. The dye laser beam was focused using a lens into the center axis of the electrode, while the OPO laser beam was not focused to cover the entire region of the dye laser beam. Laser-induced fluorescence (LIF) from the focus of the dye laser beam was collected to the entrance slit of a monochromator using a lens with image magnification of 1:1, and was detected using a photomultiplier tube. The size of the entrance slit of the monochromator was adjusted to 30  $\mu\text{m} \times 10 \text{ mm}$ . The electric signal from the photomultiplier tube was averaged using a boxcar integrator for 128 laser shots. The wavelength of the OPO laser was scanned with a step of 3 pm corresponding to a scan rate of 13.5 pm/min. The strengths of the electric fields were determined by observing the Stark spectra of Rydberg states with principal quantum numbers of 21–42. The detection limit of the electric field was 3 V/cm, which was improved from 6 V/cm in the previous article by examining the Stark effect in weak electric field precisely.

The measurement was repeated in the high-density (inductively coupled) mode and the low-density (capacitively coupled) mode of the plasma source. The high-density mode was obtained at a rf power of 100 W and a gas pressure of 5 mTorr. The low-density mode was obtained at a rf power of 40 W and a gas pressure of 10 mTorr. The electron density and the electron temperature of the high-density mode were  $3 \times 10^{10} \text{ cm}^{-3}$  and 4.0 eV, respectively, while in the low-density mode, they were  $2 \times 10^9 \text{ cm}^{-3}$  and 3.7 eV, respectively. The plasma potentials in the high-density and low-density modes were 20 and 23 V, respectively, with respect to the ground potential. These plasma parameters were mainly measured using a Langmuir probe, while the electron density in the low-density mode was calibrated using a plasma absorption probe (PAP).<sup>6</sup>

Figures 2(a) and 2(b) show the dip spectra observed in the high-density mode discharge at distances of 0.6 and 5 mm from the electrode, respectively. The spectrum shown in Fig. 2(a) has an oscillation structure, which is due to Stark splitting in the presence of an electric field. In addition, as marked in Figs. 2(a) and 2(b), forbidden transitions from the  $4p[3/2]_2$  to  $np$  states become observable by Stark mixing, and the positions of the  $np$  states or the distances between the  $np$  states and the  $(n-1)d[3/2]_2^0$  and  $(n-1)d[1/2]_2^0$  states are sensitive functions of an electric field. The strength of electric field [324 V/cm in Fig. 2(a) and 10.5 V/cm in Fig. 2(b)] was deduced from the magnitude of Stark shift and/or the intervals of the Stark splitting components indicated by the dotted lines in Fig. 2(a). The details for deducing electric fields from dip spectra will be reported elsewhere.

Figure 3 shows the distribution of the electric field strength in front of the electrode together with the results of theoretical calculation mentioned below. The axes are shown by real values and normalized ones using the electron temperature  $T_e$  and the Debye length  $\lambda_D$ . The horizontal error

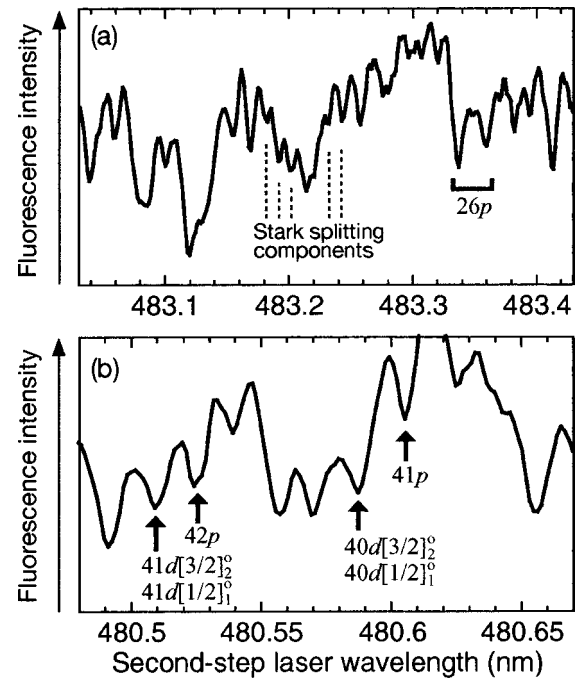


FIG. 2. Typical Stark spectra obtained in high-density mode discharge.

bars indicate the spatial resolution of the measurement, which is mainly determined by the ambiguity in the position of the movable electrode. The vertical error bars are evaluated from the linewidths of the tunable lasers and the ambiguity in the positions of energy levels in the reference spectra<sup>5</sup> examined in the plasma-free condition.

The distribution of the electric field shown in Fig. 3(a) was observed in the high-density mode when the electrode was biased at  $-50 \text{ V}$  with respect to the ground potential. As shown in the figure, the strength of the electric field decayed

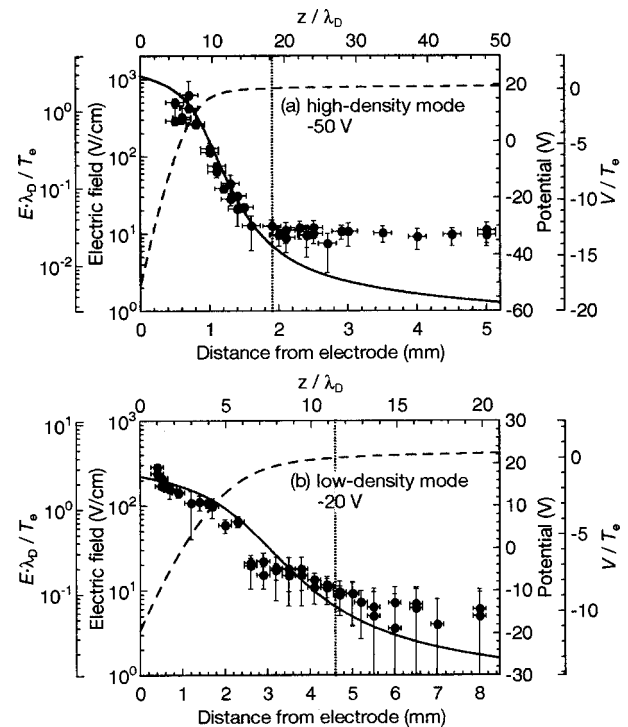


FIG. 3. Comparison between the experimental results and the theoretical electric fields.

steeply below 20 V/cm within a distance of 1.5 mm from the biased electrode. The steep decay was followed by a long tail component. Owing to the sensitive detection limit, we succeeded in measuring weak electric fields in the tail component. The electric field at a distance of 3–5 mm from the electrode was  $\sim 10$  V/cm. Figure 3(b) was obtained in the low-density mode when the electrode potential was  $-20$  V. As shown in the figure, the decay of the electric field strength was gentle in the low-density discharge, which was reasonable since the Debye length in the low-density discharge was approximately four times thicker than that in the high-density discharge. The distribution shown in Fig. 3(b) was also composed of the steep-decay part (0.4–2.5 mm) and the tail component (2.5–8 mm). A gradual decrease in the electric field strength was observed in the low-density mode in the tail component.

Kono has studied the sheath structure in electronegative plasmas using a fluid model.<sup>7–9</sup> In the present work, we compared the experimental results with theoretical electric fields obtained from a fluid model similar to that in Ref. 9 (but without including the effect of negative ions). The fluid model was composed of a momentum balance equation, a flux continuity equation in the ion flow, and Poisson's equation; electrons are assumed to be in Boltzmann equilibrium. Elastic collision and charge exchange collision were taken into account in the momentum balance equation. In the flux continuity equation, the production of ions due to electron impact ionization was considered. The collision frequencies of these elementary processes were evaluated by using the actual cross section data in the literature.<sup>10,11</sup> The procedure for obtaining boundary conditions in solving the equations has been described in the previous article.<sup>9</sup>

The solid and dashed curves shown in Fig. 3 represent the distributions of the theoretical electric fields and the theoretical electric potential, respectively. The origins of the normalized potential axes are the potentials at the sheath edge. The positions of the sheath edge are indicated by the vertical dotted lines in the figures. In this article, the conventional definition was used for the sheath edge, that is, the velocity of ion fluid has the Bohm velocity at the sheath edge. As shown in the figures, the strengths and the distributions of the electric fields in the sheath region observed experimentally were consistent with the theoretical results. On the other hand, the strengths of the electric fields in the presheath regions were higher than the theoretical electric field strengths. The reason for the discrepancy has not been

understood well. However, it is suggested that the discrepancy is partly attributed to the nonuniform distributions of the plasma potential and the electron temperature from the power-deposition area near the rf antenna toward the downstream plasmas. Another explanation for the discrepancy is the influence of microfield,<sup>12,13</sup> which may change the spectra of high Rydberg states.

In summary, we have applied laser-induced fluorescence-dip spectroscopy to Ar atoms, and have demonstrated the measurements of the distributions of the electric fields in the sheath and presheath regions of low-pressure Ar plasmas. Owing to the sensitive detection limit of LIF dip of Ar, we have succeeded in measuring weak electric fields in the presheath region and the interface region between sheath and presheath. The distributions of the electric fields measured experimentally have been compared with theoretical results based on a simple fluid model. We will continue the measurements of electric fields in various plasmas by making the best use of the high sensitivity and the universality of LIF dip of Ar.

This work was carried out under the leadership of the late Professor Kiyoshi Kadota. The authors would like to express their gratitude to him. The authors also would like to thank Dr. Nakamura (Chubu University, Japan) for the electron density measurement using PAP. This work was supported by a Grant-in-Aid for Scientific Research B (No. 13480124) from the Japan Society for the Promotion of Science.

<sup>1</sup>D. K. Doughty and J. E. Lawler, *Appl. Phys. Lett.* **45**, 611 (1984).

<sup>2</sup>K. E. Greenberg and G. A. Hebner, *Appl. Phys. Lett.* **63**, 3282 (1993).

<sup>3</sup>J. B. Kim, K. Kawamura, Y. W. Choi, M. D. Bowden, K. Muraoka, and V. Helbig, *IEEE Trans. Plasma Sci.* **26**, 1556 (1998).

<sup>4</sup>U. Czarnetzki, D. Luggenhölscher, and H. F. Döbele, *Phys. Rev. Lett.* **81**, 4592 (1998).

<sup>5</sup>K. Takizawa, K. Sasaki, and K. Kadota, *Jpn. J. Appl. Phys., Part 2* **41**, L1285 (2002).

<sup>6</sup>H. Kokura, K. Nakamura, I. Ghanashev, and H. Sugai, *Jpn. J. Appl. Phys., Part 1* **38**, 5262 (1999).

<sup>7</sup>A. Kono, *J. Phys. D* **32**, 1357 (1999).

<sup>8</sup>A. Kono, *J. Phys. D* **34**, 1083 (2001).

<sup>9</sup>A. Kono, *J. Phys. D* **36**, 465 (2003).

<sup>10</sup>R. S. Robinson, *J. Vac. Sci. Technol.* **16**, 185 (1979).

<sup>11</sup>H. C. Straub, P. Renault, B. G. Lindsay, K. A. Smith, and R. F. Stebbings, *Phys. Rev. A* **52**, 1115 (1995).

<sup>12</sup>U. Czarnetzki, V. Kadetov, D. Luggenhölscher, and H. F. Döbele, *Proceedings of the 10th International Symposium Laser-Aided Plasma Diagnostics* (Fukuoka, Japan, 2001), p.15.

<sup>13</sup>V. N. Ochkin, S. Y. Savinov, S. N. Tskhai, U. Czarnetzki, V. Schulz-von der Gathen, and H. F. Döbele, *IEEE Trans. Plasma Sci.* **26**, 1502 (1998).